

Research article

Open Access

Roles of the creatine kinase system and myoglobin in maintaining energetic state in the working heart

Fan Wu and Daniel A Beard*

Address: Biotechnology and Bioengineering Center, Department of Physiology, Medical College of Wisconsin, Milwaukee, Wisconsin 53226, USA

Email: Fan Wu - fwu@mcw.edu; Daniel A Beard* - dbeard@mcw.edu

* Corresponding author

Published: 19 February 2009

Received: 23 July 2008

BMC Systems Biology 2009, **3**:22 doi:10.1186/1752-0509-3-22

Accepted: 19 February 2009

This article is available from: <http://www.biomedcentral.com/1752-0509/3/22>

© 2009 Wu and Beard; licensee BioMed Central Ltd.

This is an Open Access article distributed under the terms of the Creative Commons Attribution License (<http://creativecommons.org/licenses/by/2.0>), which permits unrestricted use, distribution, and reproduction in any medium, provided the original work is properly cited.

Abstract

Background: The heart is capable of maintaining contractile function despite a transient decrease in blood flow and increase in cardiac ATP demand during systole. This study analyzes a previously developed model of cardiac energetics and oxygen transport to understand the roles of the creatine kinase system and myoglobin in maintaining the ATP hydrolysis potential during beat-to-beat transient changes in blood flow and ATP hydrolysis rate.

Results: The theoretical investigation demonstrates that elimination of myoglobin only slightly increases the predicted range of oscillation of cardiac oxygenation level during beat-to-beat transients in blood flow and ATP utilization. In silico elimination of myoglobin has almost no impact on the cytoplasmic ATP hydrolysis potential (ΔG_{ATPase}). In contrast, disabling the creatine kinase system results in considerable oscillations of cytoplasmic ADP and ATP levels and seriously deteriorates the stability of ΔG_{ATPase} in the beating heart.

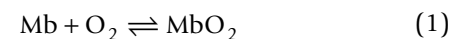
Conclusion: The CK system stabilizes ΔG_{ATPase} by both buffering ATP and ADP concentrations and enhancing the feedback signal of inorganic phosphate in regulating mitochondrial oxidative phosphorylation.

Background

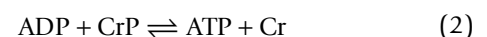
The working heart relies on uninterrupted supplies of oxygen and substrates to maintain its normal function under different workloads [1,2]. However, during the systole the heart muscle contracts and the coronary blood flow is greatly reduced; while during the diastole the heart muscle relaxes, and the coronary blood flow approaches a maximum [1,2].

Abundant myoglobin and creatine pools exist in cardiac tissue, and their roles have been extensively studied [3-8].

The O₂-Mb binding reaction is



and the creatine kinase reaction is



Myoglobin may work as an oxygen buffer [6,9], facilitate oxygen diffusion at low cellular oxygen tension [10-12], and/or catalyze chemical reactions (such as NO scavenging) [13-15]. Similarly, the creatine kinase system may either buffer cellular ATP levels or facilitate ATP diffusion inside myocytes [7,8,16].

Under normoxic conditions facilitated diffusion of oxygen by oxy-myoglobin is not expected to play a significant role in oxygen transport in the myocardium [6,17,18]. Therefore we consider only the oxygen storage function of myoglobin in this computational study. The importance of CK-facilitated high-energy phosphate transport depends on diffusion path length and diffusivity of ATP and ADP in cardiomyocytes [7]. Since the myofibrils generally have small diameters (1–2 μm) and are surrounded by dense mitochondria, it is possible that CK-facilitated transport does not play a significant role in vivo either [7]. The CK-shuttle theory of Saks et al. [8,19,20] requires restricted intracellular diffusivity of ADP, for which there is no unambiguous experimental evidence. In this study the buffering role of the CK system is investigated, and CK-facilitated diffusion of high-energy phosphate is not considered.

Here, the roles of myoglobin and creatine phosphate in buffering the energy state (i.e., ATP hydrolysis potential) in the working heart are investigated using a multi-scale computer model integrating cellular metabolism with oxygen transport in the cardiac tissue [21,22]. The cellular metabolism model was adopted from a recently-published computer model of energetic metabolism of cardiac mitochondria [23]. The metabolic model is integrated with a model of oxygen transport accounting for heterogeneous oxygenation in cardiac tissue [21].

To examine roles of myoglobin and the CK system, simulations were performed for the normal model (control) and models with myoglobin and CK not active. The simulations demonstrate that the effects of myoglobin on metabolite levels and cytoplasmic ATP hydrolysis potential are barely discernible in the working heart. In contrast, the CK system plays an essential role in maintaining the energetic state in the heart.

Methods

A computational model previously described and validated [21] is applied to simulate metabolic responses of the beating heart to various workloads. The model components are illustrated in Figure 1. A previously developed and validated axially-distributed oxygen transport models is used to simulate oxygen transport in the cardiac tissue (illustrated in Figure 1). The axially-distributed oxygen transport model is divided into three regions including capillaries, interstitial space, and myocardium, where oxygen binds hemoglobin in red blood cells in capillaries, diffuses into myocardium, and is consumed in mitochondria. A detailed cellular metabolism model is integrated with the multiple-pathway model of oxygen transport, as illustrated in Figure 1. For detailed descriptions of the model, see the Methods and Appendices sections in Wu et al. [21,23]. All model parameters and initial conditions

are the same as those used in our previous work [21]. To reduce computational cost, we modify the model described in Reference [21] by reducing the number of the pathways from ten to one and assuming that the ATP hydrolysis rate remains constant during systole. The resulting single-pathway transport model lacks the capability of the multiple-pathway model to characterize the heterogeneous oxygenation in cardiac tissue under ischemia, but still provides a valid and reliable description of oxygenation under normal physiological conditions as simulated in this work [21,22]. The nomenclature and symbols used in this paper are defined in Table 1. Detailed descriptions of the computational model components are included in Additional file 1.

Data on blood flow and heart rate under different oxygen consumption rates are collected from a series of experimental data on in vivo dog hearts reported by Zhang et al. in Figure 2[24-29]. Here measured blood flow and heart rate are shown at a number of measured oxygen consumption rates. At the mean resting conditions baseline work rate ($\text{MVO}_2 = 3.5 \mu\text{mol min}^{-1} (\text{g tissue})^{-1}$ and $\text{JATPase} = 0.36 \text{ mmol sec}^{-1} (\text{liter cell})^{-1}$) blood flow and heart rate are $0.76 \text{ ml min}^{-1} (\text{g tissue})^{-1}$ and $137 \text{ beats min}^{-1}$, respectively. At the average maximum observed work rate ($\text{MVO}_2 = 10.7 \mu\text{mol min}^{-1} (\text{g tissue})^{-1}$ and $\text{JATPase} = 1.2 \text{ mmol sec}^{-1} (\text{liter cell})^{-1}$) blood flow and heart rate are $2.31 \text{ ml min}^{-1} (\text{g tissue})^{-1}$ and $219 \text{ beats min}^{-1}$, respectively. The data in Figure 2 are used to determined relationships between rate of oxygen consumption and average blood flow and heart rate. The linear relationships are $G = 0.2146 \text{ MVO}_2 + 0.0093$ and $\text{HR} = 11.415 \text{ MVO}_2 + 96.95$, where MVO_2 is expressed in units of $\mu\text{mol min}^{-1} (\text{g tissue})^{-1}$, G is flow in units of $\text{ml min}^{-1} (\text{g tissue})^{-1}$, and HR is heart rate in units of beats min^{-1} .

To simulate dynamic blood flow and ATP hydrolysis activity on the beat-to-beat time scale in the working heart, square waves of blood flow and ATPase activity are used, as shown in Figure 3A and 3B. This assumes that blood flow totally stops and ATP consumption rate is nonzero only during systole. Conversely, blood flow is nonzero and ATP consumption is zero during diastole. Experimental observations on coronary blood flow and left ventricular pressure show that neither coronary blood flow nor ATP consumption goes to zero during the heart cycle [30]. Thus the square waves of blood flow and ATP hydrolysis activity shown in Figure 3A and 3B simulate an extreme mismatch between blood flow and ATP consumption. This simplified model allows us to probe a theoretical upper limit on the range of oscillation of concentrations of biochemical reactants.

Oxygen tension in the three compartments (capillaries, interstitial space, and myocardium), mitochondrial mem-

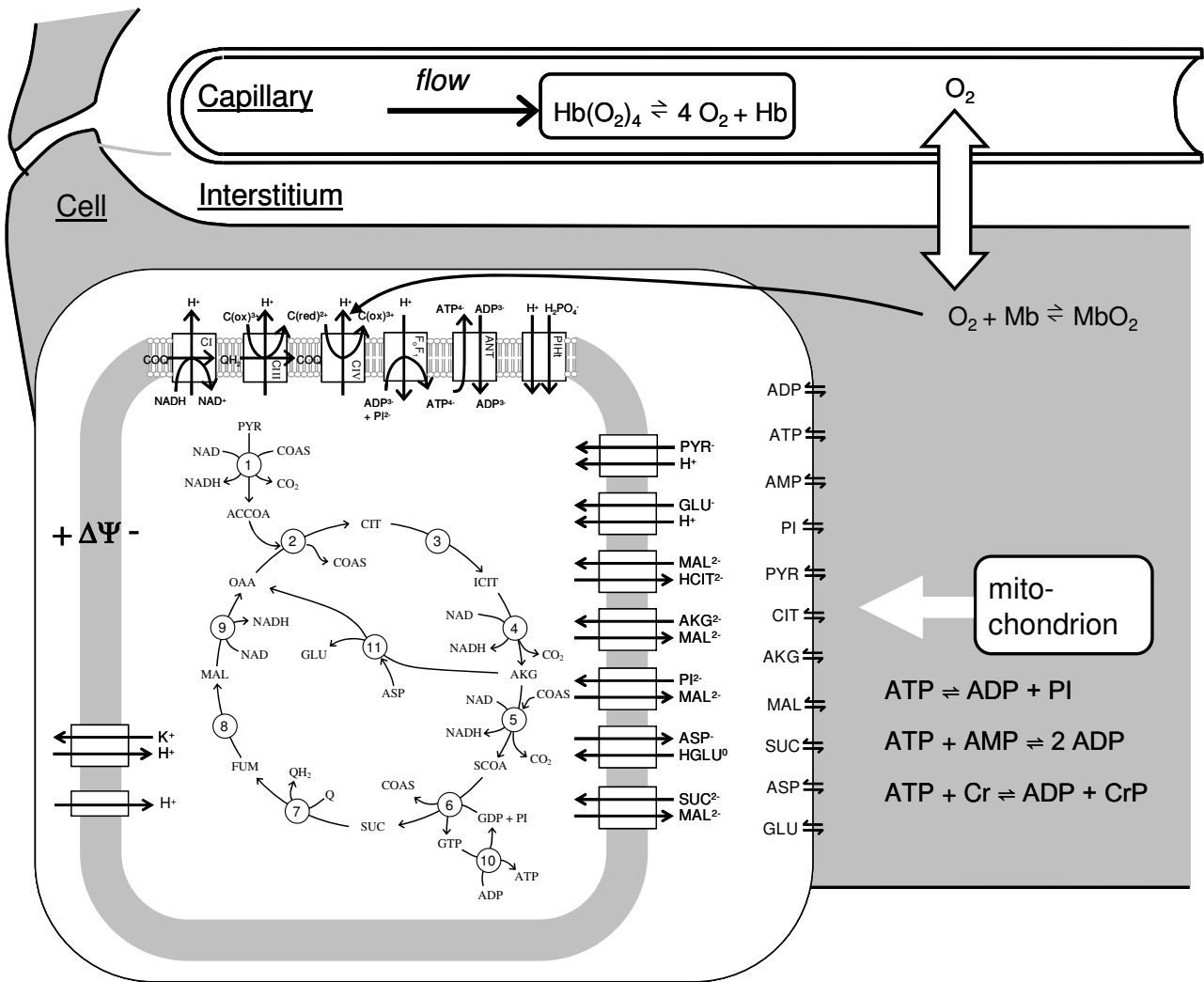


Figure 1
Diagram of model used to simulate cardiac tissue oxygen transport and energy metabolism. Oxygen is transported via advection in capillaries, diffuses into cardiomyocytes from capillaries through interstitium, and is reduced into water via the complex IV reaction in mitochondria. Cellular energy metabolism is simulated by a computer model of mitochondrial tricarboxylic acid cycle, oxidative phosphorylation, metabolite transport, and electrophysiology [23].

brane potential, and concentrations of metabolites are obtained from model simulations. Myoglobin saturation is computed from oxygen tension in myocardium ($P_{O_2, cell}$) as

$$S_{Mb} = \frac{P_{O_2, cell}}{P_{O_2, cell} + P_{50, Mb}}, \quad (3)$$

where $P_{50, Mb}$ is the half-saturation partial pressure for the oxygen-myoglobin binding, 2.39 mmHg [22].

The free energy potential of ATP hydrolysis is computed from

$$\Delta G_{ATPase} = \Delta G_{ATPase}^{\circ} + RT \ln \frac{[ADP]_c [Pi]_c}{[ATP]_c}, \quad (4)$$

where $\Delta G_{ATPase}^{\circ} = -34.89 \text{ kJ mol}^{-1}$ [31] at ionic strength $I = 0.17 \text{ M}$, and temperature $T = 310.15 \text{ K}$, and R is the gas constant equal to $8.314 \text{ kJ mol}^{-1} \text{ K}^{-1}$. The subscript "c" denotes cytoplasm.

Table 1: Nomenclature

Symbol	Definition	Units
C	Buffer capacity of the CK system	$\text{mol}^2 \text{kJ}^{-1}$
C_{Mb}	Myoglobin concentration	μM
CR_{tot}	Total creatine pool in myocardium	$\text{mmol} (\text{l cytoplasm water})^{-1}$
ΔG_{ATPase}	Cytoplasmic ATP hydrolysis potential	kJ mol^{-1}
$ \Delta \bar{G}_{\text{ATPase}} $	Average magnitude of cytoplasmic ATP hydrolysis potential	kJ mol^{-1}
$\Delta G_{\text{ATPase}}^{\circ'}$	Transformed Gibbs free energy of ATP hydrolysis	kJ mol^{-1}
$\Delta \Psi$	Mitochondrial inner membrane potential	mV
G	Blood flow	$\text{ml min}^{-1} (\text{g tissue})^{-1}$
HR	Heart rate	beats min^{-1}
I	Ionic strength	M
J_{ANT}	Mitochondrial ANT transport flux	$\text{mmol sec}^{-1} (\text{liter mito})^{-1}$
J_{ATPase}	Cytoplasmic ATP consumption rate	$\text{mmol sec}^{-1} (\text{liter cell})^{-1}$
MVO_2	Oxygen consumption rate	$\mu\text{mol min}^{-1} (\text{g tissue})^{-1}$
$P_{\text{O}_2, \text{cell}}$	Partial oxygen pressure in myocardium	mmHg
$P_{50, \text{Mb}}$	Half-saturation partial pressure for the oxygen-myoglobin binding	mmHg
R	Gas constant	$\text{kJ mol}^{-1} \text{K}^{-1}$
S_{Mb}	Myoglobin saturation	unitless
T	Temperature	K
t	Time	second

Oxygen-myoglobin binding is assumed to be maintained in equilibrium in the tissue model. The kinetics of the CK reaction is governed according to the model described in Reference [21]. Molecular diffusion of creatine, phosphocreatine, and myoglobin are not included in the model (see Reference [21]). Therefore putative roles of oxy-myoglobin and phosphocreatine are not explored in this work.

Results

To understand the roles of myoglobin and the creatine kinase system as buffers in maintaining the energetic state in the heart, we simulate transient responses and steady states of cardiac energetics under different cardiac workloads in three systems: (1) a normal system with both the normal myoglobin level and creatine kinase activity; (2) a system without myoglobin (no-Mb system); (3) a system with zero creatine kinase activity (no-CK system). The fol-

lowing analyses demonstrate the importance of the CK system in stabilizing energetic states in the beating heart. In the normal system, the myoglobin concentration (C_{Mb}) is set to be a physiologically reasonable value $200 \mu\text{M}$ [32], and the creatine kinase activity is set to be an arbitrary large value to ensure that the CK reaction is rapid enough to remain near equilibrium [33]. C_{Mb} is reduced to zero in the no-Mb system, and the creatine kinase activity is set to be zero in the no-CK system.

Transient cardiac energetics in responses to a step change of workload

The normal system

Figure 4 illustrates transient changes of myoglobin saturation level (S_{Mb}), phosphate metabolite levels, cytoplasmic ATP hydrolysis potential (ΔG_{ATPase}), mitochondrial inner membrane potential ($\Delta \Psi$), and mitochondrial ANT transport flux (J_{ANT}), following a step change of cardiac work-

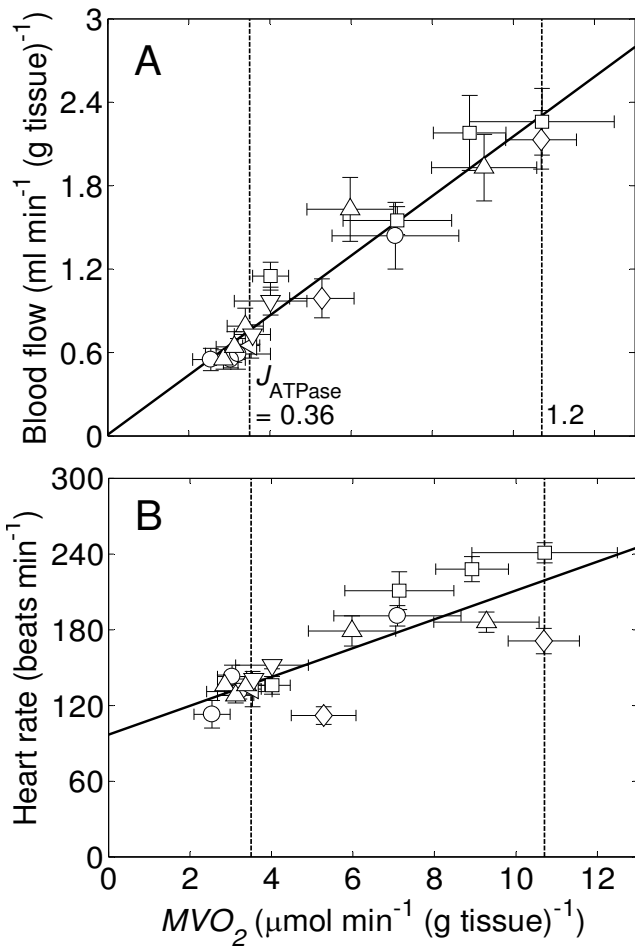


Figure 2
Relationships between oxygen consumption rate (MVO_2), blood flow (F), and heart rates (HR) in cardiac tissue. (A.) Plot of blood flow against oxygen consumption rate. (B.) Plot of heart rate against oxygen consumption rate. Experimental data are obtained from the following sources: \circ , Zhang et al. [25]; $\tilde{\alpha}$, Zhang et al. [24]; \diamond , Gong et al. [26]; \triangle , Ochiai et al. [27]; $\acute{\alpha}$, Gong et al. [28]; \square , Bache et al. [29]. The relationship between J_{ATPase} , the ATP hydrolysis rate, and MVO_2 is predicted by the computer model. The solid lines represent the best fits to the data: $G = 0.2146 MVO_2 + 0.0093$ with R-squared value (R^2) = 0.9414 (in Figure A) and $HR = 11.415 MVO_2 + 96.95$ with $R^2 = 0.6892$ (in Figure B). The vertical dashed lines mark baseline ($J_{ATPase} = 0.36$ mmol s^{-1} (l cell) $^{-1}$) and high MVO_2 ($J_{ATPase} = 1.2$ mmol s^{-1} (l cell) $^{-1}$). J_{ATPase} is expressed in units of mmol s^{-1} (l cell) $^{-1}$, G in units of ml min^{-1} (g tissue) $^{-1}$, and HR in units of beats min^{-1} .

load and coronary blood flow (shown in Figure 3) in the normal system. The ANT transport flux is the rate at which ATP is transported from the mitochondrial matrix to the cytoplasm in exchange for ADP. When the step change in work rate occurs at time $t = 6$ seconds, these variables move from their baseline steady state values to approach new steady-state values at the maximal workload after

about 20 seconds. Average S_{Mb} decreases from 0.94 to 0.91, average $[ATP]_c$ remains almost constant (slightly decreasing from ~ 9.66 to ~ 9.64 mM), average $[CrP]_c$ decreases from ~ 23.4 to ~ 19.5 mM, average $[Pi]_c$ increases from ~ 0.28 to ~ 2.1 mM, average $[ADP]_c$ increases from ~ 42 to ~ 62 μM , average $-\Delta G_{ATPase}$ decreases from ~ 70.2 to ~ 63.5 kJ mol^{-1} , average $\Delta\Psi$ decreases from ~ 180 to ~ 174 mV, and average J_{ANT} increases from 0.36 to 1.2 mmol s^{-1} (l cell) $^{-1}$. The range of oscillation of the variables in S_{Mb} , $[ATP]_c$, $[CrP]_c$, $[Pi]_c$, $[ADP]_c$ and J_{ANT} increases slightly, but interestingly, the oscillations of $-\Delta G_{ATPase}$ and $\Delta\Psi$ slightly decrease, implying that despite elevated instability of oxygenation and phosphate metabolite levels, energetic stability is slightly increased with increasing work rate.

The no-Mb system

To investigate the effects of myoglobin on cardiac energetics, simulations of the no-Mb system following the same protocols used above for the normal system were performed. Comparing results from the no-Mb system (shown in Figure 5) with those of the normal system (Figure 4), it is apparent that the myoglobin buffering has little impact on the temporal fluctuations. The oscillations in S_{Mb} are only slightly higher for the no-Mb system compared to the control. These fluctuations do not impact other energetic variables because the corresponding cellular oxygen tension remains above 15 mmHg at the maximum work rate and does not limit oxidative capacity in the heart [18].

The no-CK system

To investigate the effects of CK buffering on the system, simulations of the no-CK system were performed using the same protocols used for the control, with the activity of creatine kinase is set to be zero for the simulations. Results illustrated in Figure 6 demonstrate the importance of the CK system in maintaining cardiac energetic state. Compared with the results in Figure 4, disabling the CK system causes considerably enhanced oscillations of S_{Mb} , $[ATP]_c$, $[Pi]_c$, $[ADP]_c$, ΔG_{ATPase} , $\Delta\Psi$, and J_{ANT} during the cardiac cycle. In addition, removing CK prevents release of Pi from creatine phosphate (CrP) in response to increases in work rate. As a result, the average $[Pi]_c$ is reduced from ~ 2.1 mM in the normal system to ~ 0.7 mM in the no-CK system at the maximum workload.

Steady-state cardiac energetics at varying workloads

The preceding transient simulations demonstrate the important role of the CK system in maintaining energetic stability in the beating heart. Next, we further explore impacts of the CK system on steady states of S_{Mb} , $[ATP]_c$, $[CrP]_c$, $[Pi]_c$, $[ADP]_c$, ΔG_{ATPase} , $\Delta\Psi$, and J_{ANT} at varying workloads by simulating steady-state metabolite levels as a function of work rate. In Figure 7, the predicted range (over the cardiac cycle) of each illustrated metabolite is

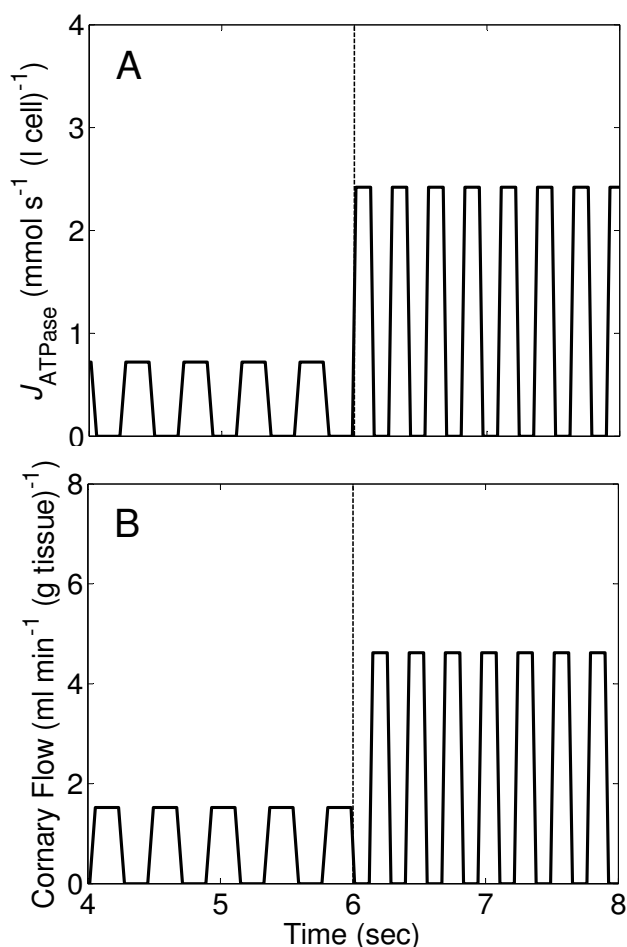


Figure 3
Temporal profiles of blood flow and cytoplasmic ATP consumption rate used as model inputs. (A.) Time course of blood flow with a step change occurs at time $t = 6$ seconds corresponding to an increase of cardiac work rate from baseline to maximum level. (B.) Time course of cytoplasmic ATP consumption rate (J_{ATPase}) with a step change from baseline to maximum work rate at $t = 6$ seconds.

plotted as a shaded region. Black regions represent simulations of the control system; gray represents simulations of the no-CK system. Upper bounds of the regions represent the maximum values of the investigated variables during a heart cycle, and down bounds represent their minimum values.

Figure 7A illustrates that the oxygenation levels in the no-CK system vary slightly more than in the control system, while average oxygenation levels in the both system are nearly identical. Figure 7B shows that $[ATP]_c$ is maintained at an almost constant level (~ 9.66 mM) without noticeable oscillations over the whole range of cardiac workload in the control system; in the no-CK system

$[ATP]_c$ oscillates over a wider range ($\sim \pm 0.2$ mM at the maximum workload), and the average $[ATP]_c$ decreases from ~ 9.66 mM at the baseline workload to ~ 9.52 mM at the maximum workload in the no-CK system. Figure 7C shows that the average $[CrP]_c$ decreases from ~ 23.4 mM at the baseline workload to ~ 19.5 mM at the maximum workload in the control system. ($[CrP]_c$ is constant in the no-CK system because of zero CK activity.) Figure 7D shows that the average $[Pi]_c$ at the maximal work rate is three-fold lower in the no-CK system than in the control system. Average $[Pi]_c$ is ~ 0.7 mM at the maximum workload in the no-CK system compared to ~ 2.1 mM in the control simulation. Figure 7E shows that $[ADP]_c$ oscillates drastically in the no-CK system, where $[ADP]_c$ varies between ~ 85 μM and ~ 270 μM at the maximum workload, compared with $[ADP]_c$ varying between ~ 60 and ~ 63 μM at the maximum workload in the control system. As shown in Figure 7F, the average values of ΔG_{ATPase} are approximately equal between the control and no-CK. However, it is apparent from the predicted ranges of oscillation that the CK system acts in stabilizing ΔG_{ATPase} in the myocardium. Over the whole range of cardiac workload, the range of oscillations of ΔG_{ATPase} is approximately four times higher in the no-CK system than in the control. Mitochondrial inner membrane potential ($\Delta\Psi$) also oscillates over in a wider range ($\sim \pm 5$ mV) in the no-CK system than in the control system ($< \pm 1.2$ mV) as shown in Figure 7G. Figure 7H shows that in both the control and the no-CK systems the average J_{ANT} at the steady state is equal to the average cytoplasmic ATP hydrolysis rates at different cardiac workloads, indicating the oxidative phosphorylation flux is able to match the cellular ATP demand in both cases. However, the oxidative ATP synthesis rate in the no-CK case oscillates over a much larger range in the no-CK case.

These results demonstrate two roles of the CK system in maintaining cardiac energetic state. The first role as a buffer has been widely appreciated [7,8,16,34]. The second role is to provide a source of increasing inorganic phosphate with increases in work rate. This allows the cardiomyocytes to maintain relatively stable ATP and ADP concentration, as illustrated in Figure 7B and 7E. Briefly, Figure 7 clearly demonstrates significant roles of the CK system in maintaining energetic stability during the heart cycles at varying cardiac workloads.

Discussion

Minor impact of myoglobin on cardiac energetics

Comparisons between Figure 4 and 5 demonstrate the oxygen-storage function of myoglobin plays minor roles in maintaining energy state of the heart in normoxic conditions. However, possible physiological roles of myoglobin may be revealed under extreme conditions. The concentration of myoglobin in the heart of most ter-

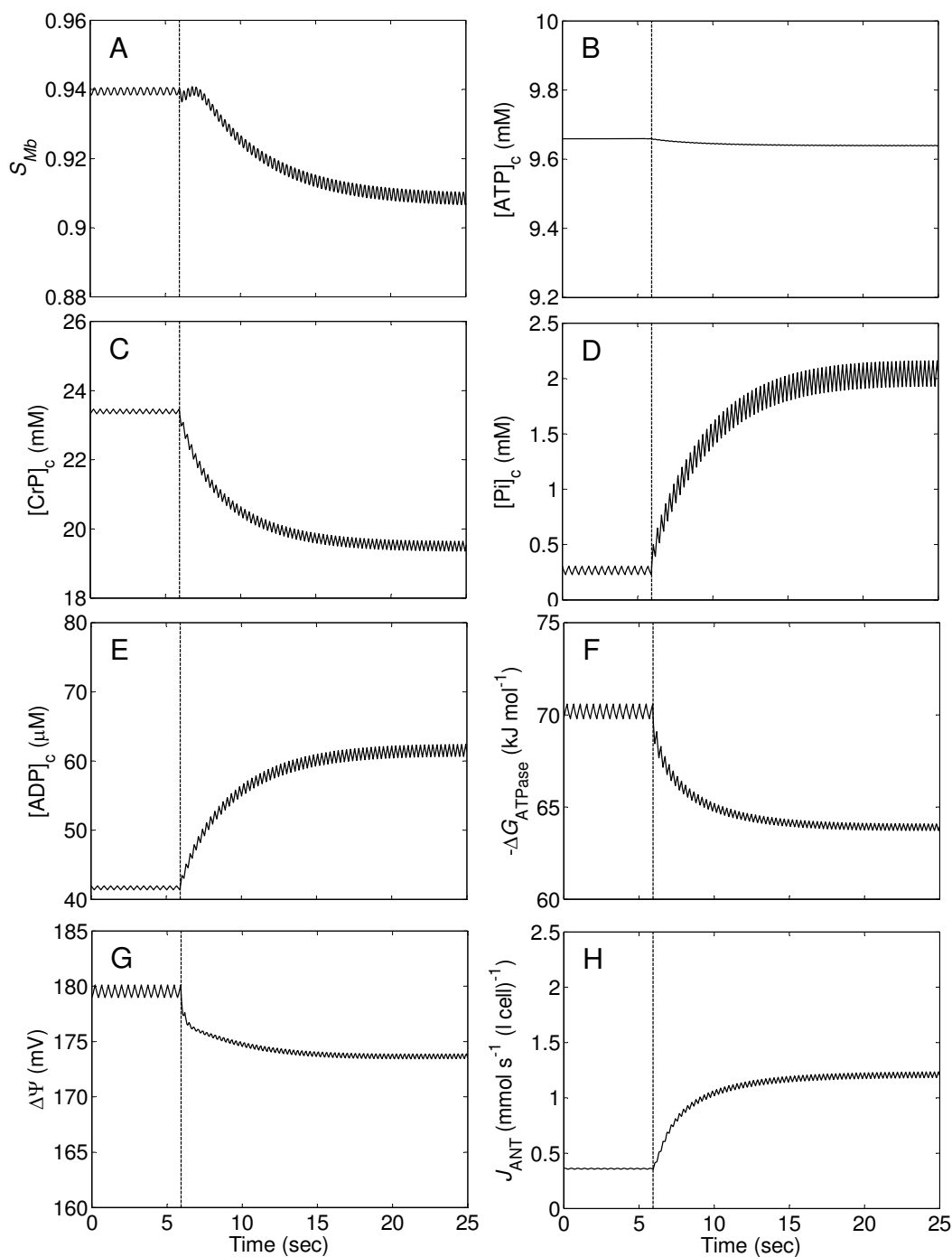


Figure 4
Transient changes of myoglobin saturation, phosphate levels, cytoplasmic ATP hydrolysis potential, mitochondrial inner membrane potential, and mitochondrial ATP production rate in the control system. (A.) Myoglobin saturation (S_{Mb}). (B.) Cytoplasmic ATP concentration ($[ATP]_c$). (C.) Cytoplasmic creatine phosphate concentration ($[CrP]_c$). (D.) Cytoplasmic inorganic phosphate concentration ($[Pi]_c$). (E.) Cytoplasmic ADP concentration ($[ADP]_c$). (F.) Cytoplasmic ATP hydrolysis potential ($-\Delta G_{ATPase}$). (G.) Mitochondrial inner membrane potential ($\Delta\Psi$). (H.) Mitochondrial ATP production rate, equal to mitochondrial adenosine nucleotide translocator flux (J_{ANT}). All variables are simulated for the time courses of the flow and ATP consumption rate in Figure 3.

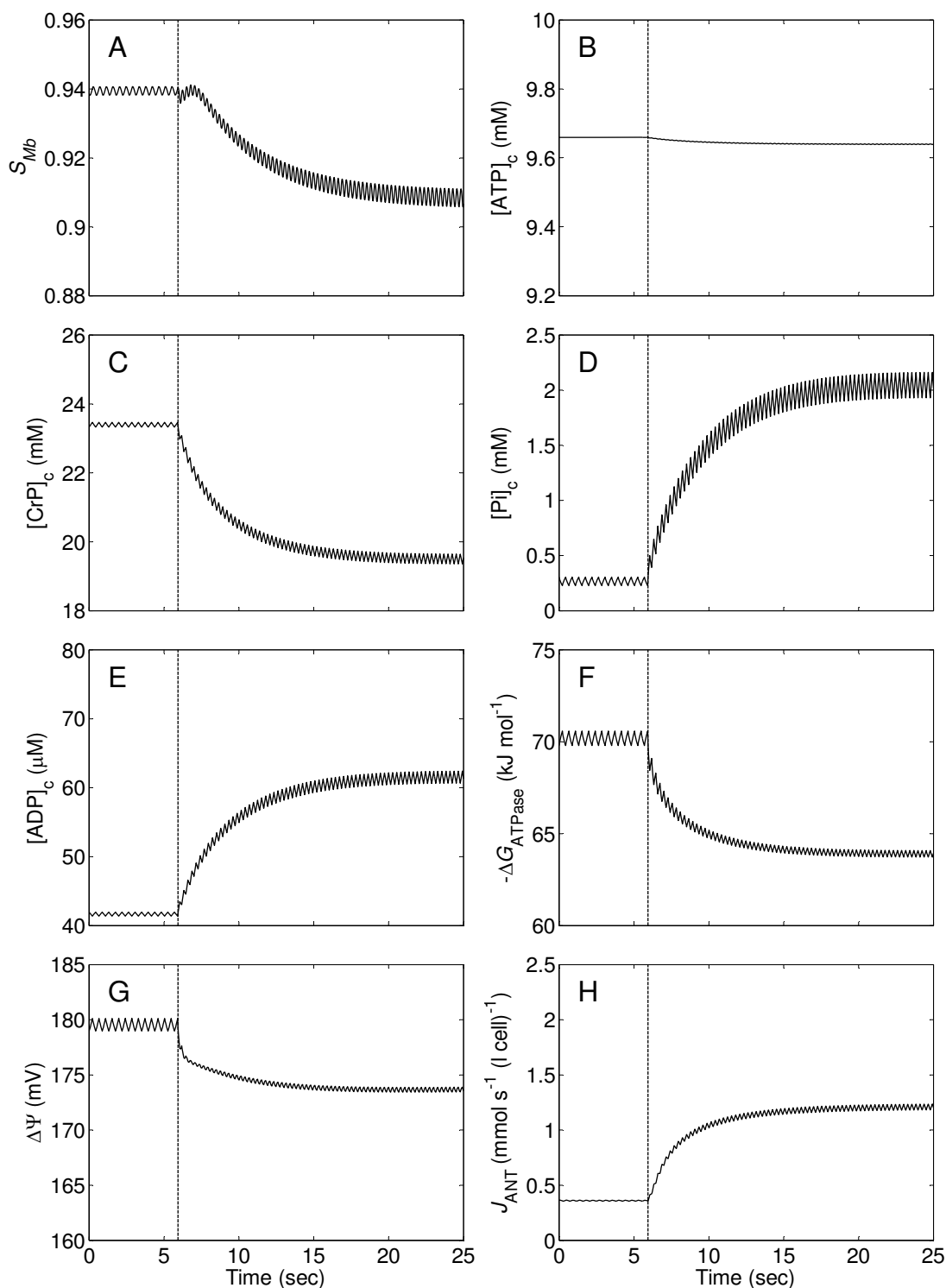


Figure 5
Transient changes of myoglobin saturation, phosphate levels, cytoplasmic ATP hydrolysis potential, mitochondrial inner membrane potential, and mitochondrial ATP production rate in the no-myoglobin (no-Mb) heart.

As for the control simulation of Figure 4, all variables are simulated for the time courses of the flow and ATP consumption rate in Figure 3.

rain mammals (e.g., rat, dog, human) is typically between 130 and 320 μM [35,36]. In the event of severe ischemia, these concentrations can only satisfy the oxygen demand of the heart for several seconds even at relatively low work rate. Comparatively, C_{Mb} level is high in diving birds and mammals (e.g., 4~5 mM in seals) [37], and may contribute to significant oxygen buffering [38].

First hypothesized over 30 years ago, the relative importance of Mb-facilitated oxygen transport has remained unclear, in part, due to conflicting experimental measurements on myoglobin diffusivity [10-12]. Early conclusions on Mb-facilitated oxygen diffusion were mainly drawn based on high estimates ($7\sim 23 \times 10^{-7} \text{ cm}^2 \text{ s}^{-1}$) of myoglobin diffusivity from in vitro measurements in dilute solution of myoglobin [4,10-12,39,40]. Using two different techniques, microinjection and fluorescence recovery after photobleaching (FRAP), Papadopoulos et al. [9,41] report that that myoglobin diffusivity is approximately $2.0 \times 10^{-7} \text{ cm}^2 \text{ s}^{-1}$ at 37°C in myocytes. Based on this low value of myoglobin diffusivity, Jurgen et al. [6] and Beard and Bassingthwaite [42] determine that the intracellular myoglobin diffusivity may be too low to provide significant facilitation of oxygen transport in well-oxygenated cardiac tissue. Jue and colleagues [43,44] report higher values of myoglobin diffusion in cardiomyocytes, $7.85 \times 10^{-7} \text{ cm}^2 \text{ s}^{-1}$ at 35°C and $4.24 \times 10^{-7} \text{ cm}^2 \text{ s}^{-1}$ at 22°C , obtained from a $^1\text{H-NMR}$ technique. However, even at these diffusivity values, myoglobin does not impact oxygen transport into the cells significantly when cellular oxygen tension is above P_{50} of myoglobin [43,44]. Similarly, Timmons et al. [45,46] report that oxygen supply does not limit oxidative ATP synthesis in rest-work transition in skeletal muscle, also implying the minor role of myoglobin in oxygen transport in oxidative striated muscle.

Myoglobin can scavenge and catalyze degradation of NO in vivo [13,47]. In addition, Rassaf et al. [14] propose that myoglobin in the heart might work as an oxygen sensor and metabolism regulator, since myoglobin can act as either an NO scavenger at high cellular P_{O_2} and an NO producer at low P_{O_2} . Since oxygenation in cardiac tissue is maintained above the P_{50} for myoglobin in normoxia, myoglobin may act as an NO scavenger under normal conditions.

The absence of myoglobin may elevate cytoplasmic NO level and consequently impacts metabolism regulation, structure, and functions in the heart. Experimental observations show that physiological performance of Mb-knockout mice is comparable to those of normal mice, but the Mb-knockout mice have significantly elevated coronary flow, coronary reserve, and capillary density compared to the control [48,49]. These differences may be

associated with elevated NO levels, resulting from reduced NO scavenging in myocytes of the Mb-knockout mice. Elevated NO may also promote angiogenesis by regulating various growth factors and increase capillary density [50-52]. Fogel et al. [53] propose that decreased myoglobin may directly affect substrate selection. For example, elevated NO level impacts substrate utilization by effecting gene expressions of the glucose transporter (GLUT4) and the peroxisome proliferator-activated receptor (PPAR α) [53]. Hence, abnormally elevated NO levels may contribute to the physiological adaptations observed in Mb-knockout mice.

In summary, our simulations predict that oxygen buffering by myoglobin in terrestrial mammals plays an insignificant role in maintaining the energy state of the beating heart. Significant changes of structure, hemodynamics, and metabolism observed in Mb-knockout mice [49,53] do not necessarily reflect compensation mechanisms for oxygen deficiency in cardiac tissue. These differences may be caused by elevated cellular NO levels in the knockout mice via various pathways [2,50-56]. In aerobic muscles, such as cardiac muscle, a large amount of mitochondria are required to provide adequate and sustained energy supply, and this high oxidative capacity is usually accompanied by abundant myoglobin, perhaps functioning primarily to scavenge NO generated by mitochondria.

Creatine kinase system is essential in stabilizing cardiac energetic state

Simulations presented in Figure 6, 7 show considerably diminished energetic stability in the no-CK system, and thus demonstrate significant roles of the creatine kinase system in maintaining normal function in the working heart. These analyses show that the CK system not only buffers cytoplasmic ATP and ADP concentrations but also enhances the Pi feedback signal in regulating mitochondrial oxidative ATP synthesis.

The CK system enhances the Pi feedback signal in regulating oxidative ATP synthesis

Mechanisms underlying regulation of cardiac energetics have been controversial for decades [19,57,58]. Our recently published work suggests that substrate feedback regulation plays an essential role in coordinating mitochondrial ATP synthesis with cellular ATP consumption [21,23,59]. As a product of ATP hydrolysis, inorganic phosphate (Pi) is a primary controller of mitochondrial oxidative ATP synthesis [23,58,60]. As shown in Figure 7 and 8, the concentration of Pi in the no-CK system increases significantly less with work rate in the control system. At the same time ADP increases significantly more in the no-CK system.

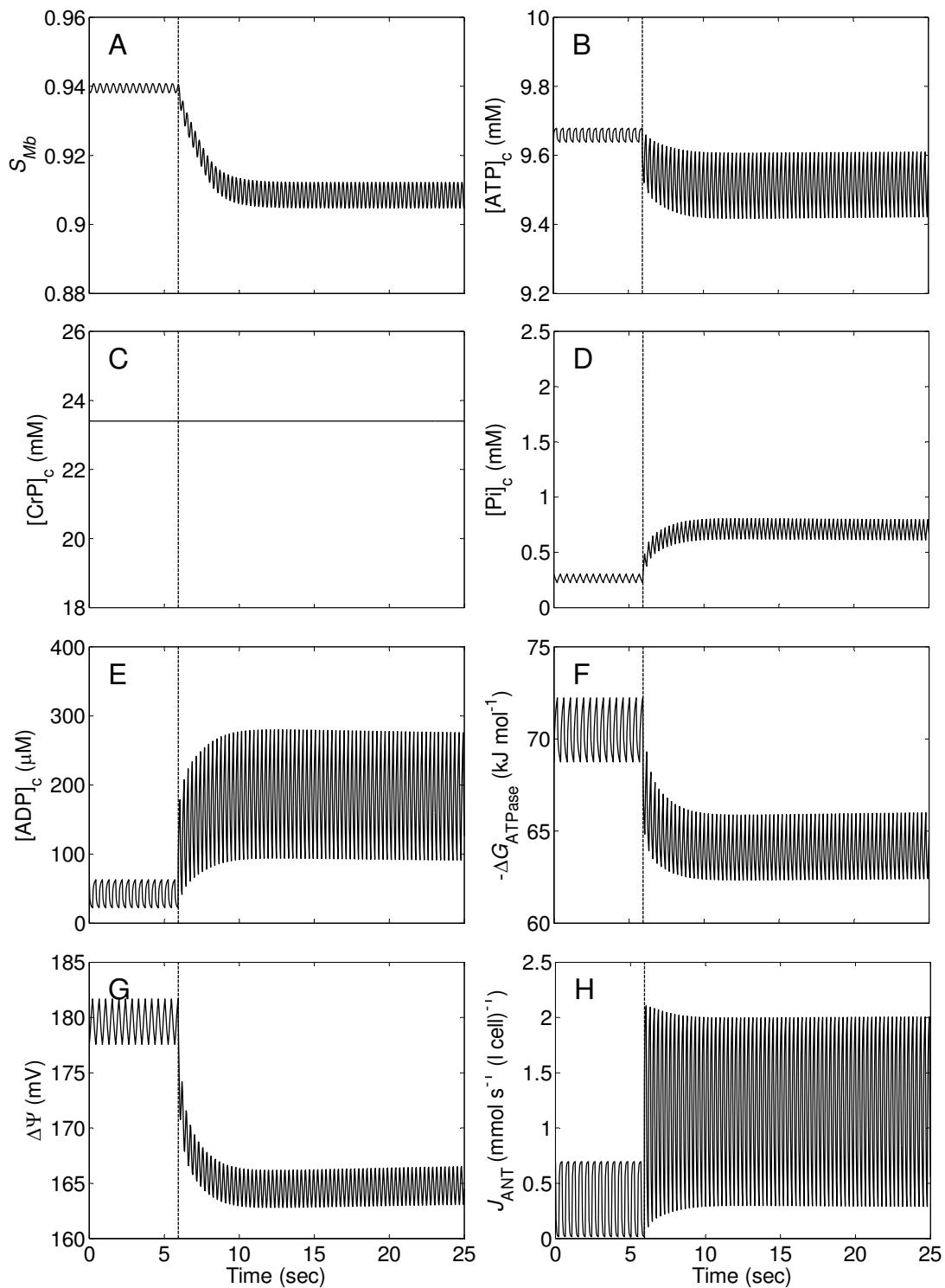


Figure 6
Transient changes of myoglobin saturation, phosphate levels, cytoplasmic ATP hydrolysis potential, mitochondrial inner membrane potential, and mitochondrial ATP production rate in the heart without creatine kinase activity (no-CK). As for the control simulation of Figure 4, all variables are simulated for the time courses of the flow and ATP consumption rate in Figure 3.

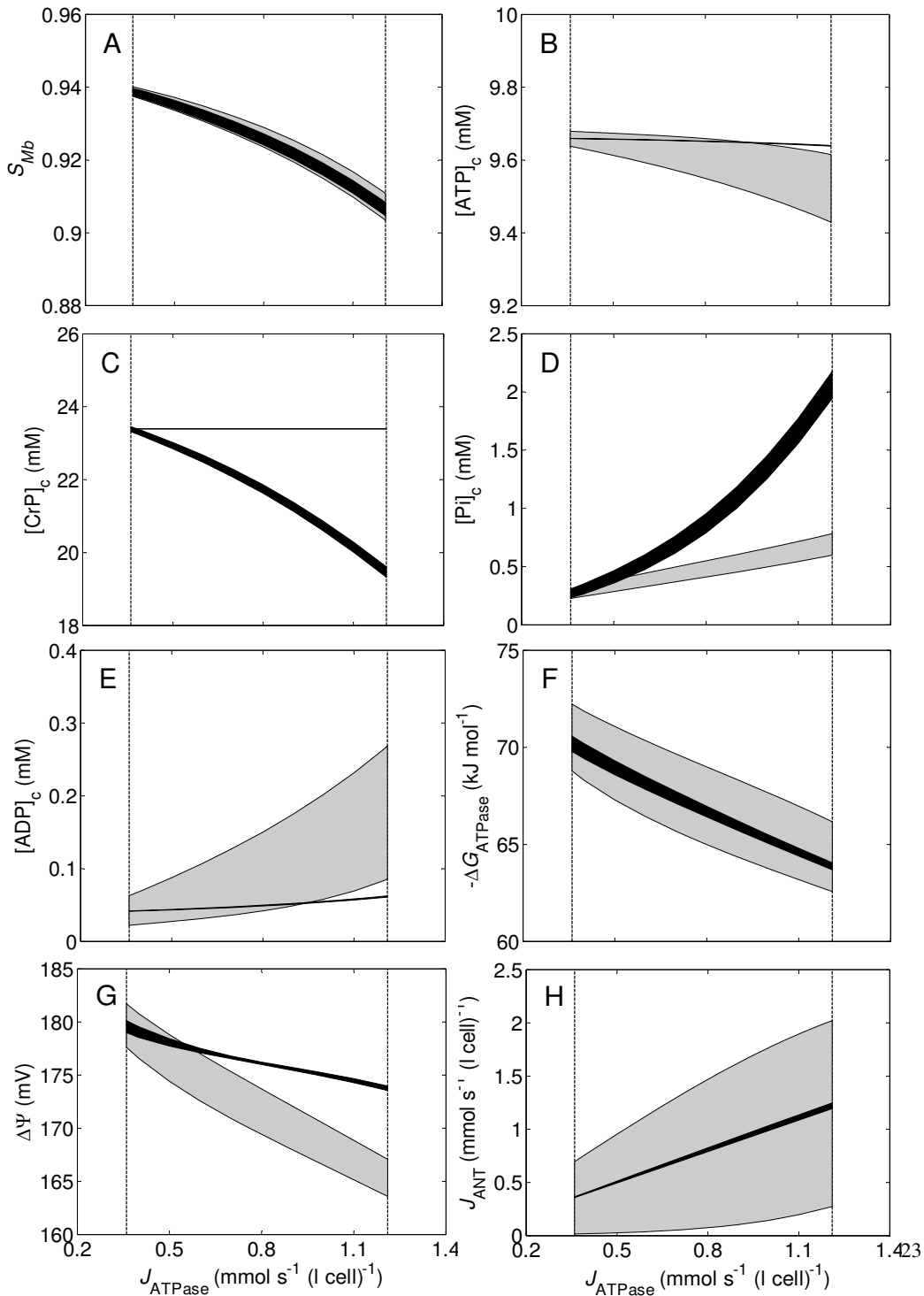


Figure 7
Steady-state myoglobin saturation, phosphate levels, cytoplasmic ATP hydrolysis potential, mitochondrial inner membrane potential, and mitochondrial ATP production rate in the control and no-CK systems. Simulated ranges of variables are shown as shaded regions, black for the control and grey for the no-CK system. The upper bounds of the regions represent the maximum values during a heart cycle at steady state, and the low bounds represent the predicted minimum values.

One way to understand the relative importance of Pi and ADP in regulating oxidative phosphorylation is to clamp their concentrations and simulate the expected impact on the phosphate metabolites. The concentrations of Pi and ADP are clamped by setting their time derivatives to be zero in the model, respectively. Results from these simulation experiments are illustrated in Figure 8. The model predictions of the control system are plotted as solid lines, and those of the no-CK system are illustrated as dashed lines. The previously obtained baseline and maximum work rates (see Methods section), 0.36 and 1.2 mmol s⁻¹ (liter cell)⁻¹, respectively, are indicated by two vertical dotted lines in the plots in Figure 8. The simulations without clamped metabolite concentrations are demonstrated in Figure 8A–C. Figure 8A shows that the magnitudes of average ΔG_{ATPase} ($|\Delta \bar{G}_{\text{ATPase}}|$) are approximately equal between the control and no-CK over the range of workload. Figure 8B illustrates that the average [Pi]_c only increases approximately two fold over the range of work rate in the no-CK system, compared to the approximately eight-fold increase in the control. Figure 8C shows that the average [ADP]_c increases approximately four fold over the range of work rate, compared to the only slight increase of the average [ADP]_c in the control. With [Pi]_c clamped at the baseline level, the model-predictions are the same in both the control and no-CK system, as shown Figure 8D–F. Figure 8D shows that $|\Delta \bar{G}_{\text{ATPase}}|$ reaches the critical value [21], 63.5 kJ mol⁻¹, at $J_{\text{ATPase}} = \sim 0.90$ mmol s⁻¹ (liter cell)⁻¹. Figure 8F shows a rapid increase of the average [ADP]_c in responses of elevated work rate. Clamping [ADP]_c impacts the simulations less significantly, as shown in Figure 8G–I. Figure 8G shows that with [ADP]_c clamped, $|\Delta \bar{G}_{\text{ATPase}}|$ reaches the critical value at $J_{\text{ATPase}} = \sim 1.04$ mmol s⁻¹ (liter cell)⁻¹ in the control, and at $J_{\text{ATPase}} = \sim 1.08$ mmol s⁻¹ (liter cell)⁻¹ in the no-CK system. With [ADP]_c clamped (Figure 8H) and with [ADP]_c free to vary (Figure 8B), Pi concentrations are higher in the control system than in the no-CK system because of a larger effective total pool of exchangeable phosphates in the control.

To summarize these findings, clamping [Pi]_c has a more significant impact on energetic stability than clamping [ADP]_c in both the control and no-CK systems. For both systems, when Pi feedback is removed from the model (by clamping [Pi]_c) the free energy of ATP hydrolysis drops more quickly with increasing work rate than in the unclamped simulations. When [ADP]_c is clamped, the

impact on the predicted energetic state is less significant than when [Pi]_c is clamped. Therefore, inorganic phosphate is a more important controller of oxidative phosphorylation than ADP in this model. Since this model is well validated against steady-state and transient in vivo data, it is likely that inorganic phosphate is a primary controller of oxidative phosphorylation in vivo.

Previous analysis of data from purified mitochondria suggests that Pi activates complex III of the respiratory chain [60]. Indeed this phenomenon is incorporated into our computational model [21,23]. When Pi level decreases in the no-CK system, the mitochondrial membrane potential (Figure 6G) is diminished, leading to increased [ADP]_c and decreased $|\Delta G_{\text{ATPase}}|$ compared to control. However, even though the Pi signal is diminished in the no-CK system, Pi remains the most important feedback signal for oxidative phosphorylation.

Saupe et al. [61] observed that as work rate increases in hearts isolated from mice with both mitochondrial and M-form CK knocked out, [Pi]_c changes little, [ADP]_c increases about three fold, and $|\Delta \bar{G}_{\text{ATPase}}|$ decreases ~ 3 kJ mol⁻¹ in these hearts compared to the control. Thus, their concentrations on ADP are qualitatively matched by our simulations, while our model predicts that [Pi]_c is lower in the no-CK system compared to the control. Since the knockout mouse cardiomyocytes show residual CK activity (40% of wild type), this animal model is not equivalent to our no-CK model. The data of Saupe et al. [61] show a decrease in CrP with increasing work rate, indicating that the CK system is potentially active in the knockout animals.

Feedback of ADP and Pi is also essential for matching oxidative ATP synthesis to cellular energy demand in skeletal muscle [23,59]. However, cytoplasmic Pi can increase to 20 mM and higher at high work rates in skeletal muscle [59] while cytoplasmic Pi is predicted to stay below 3 mM at maximal work rate in the heart [21]. Furthermore, the cytoplasmic Pi concentration in resting slow oxidative soleus muscle is in the range of 5 mM [62]. Therefore even at rest, the Pi concentration is well above the predicted regulatory feedback range for cardiac muscle. We would expect that ADP acts as an important physiological feedback signal in those muscles, as has been established [63,64].

Analysis of the energy buffering role of the CK system

A simple electrical analog model of Meyer [65] can be used to analyze the buffering role of the CK system in the cardiac energetics. In this model, the buffer capacity of the CK system is computed by the following relationship:

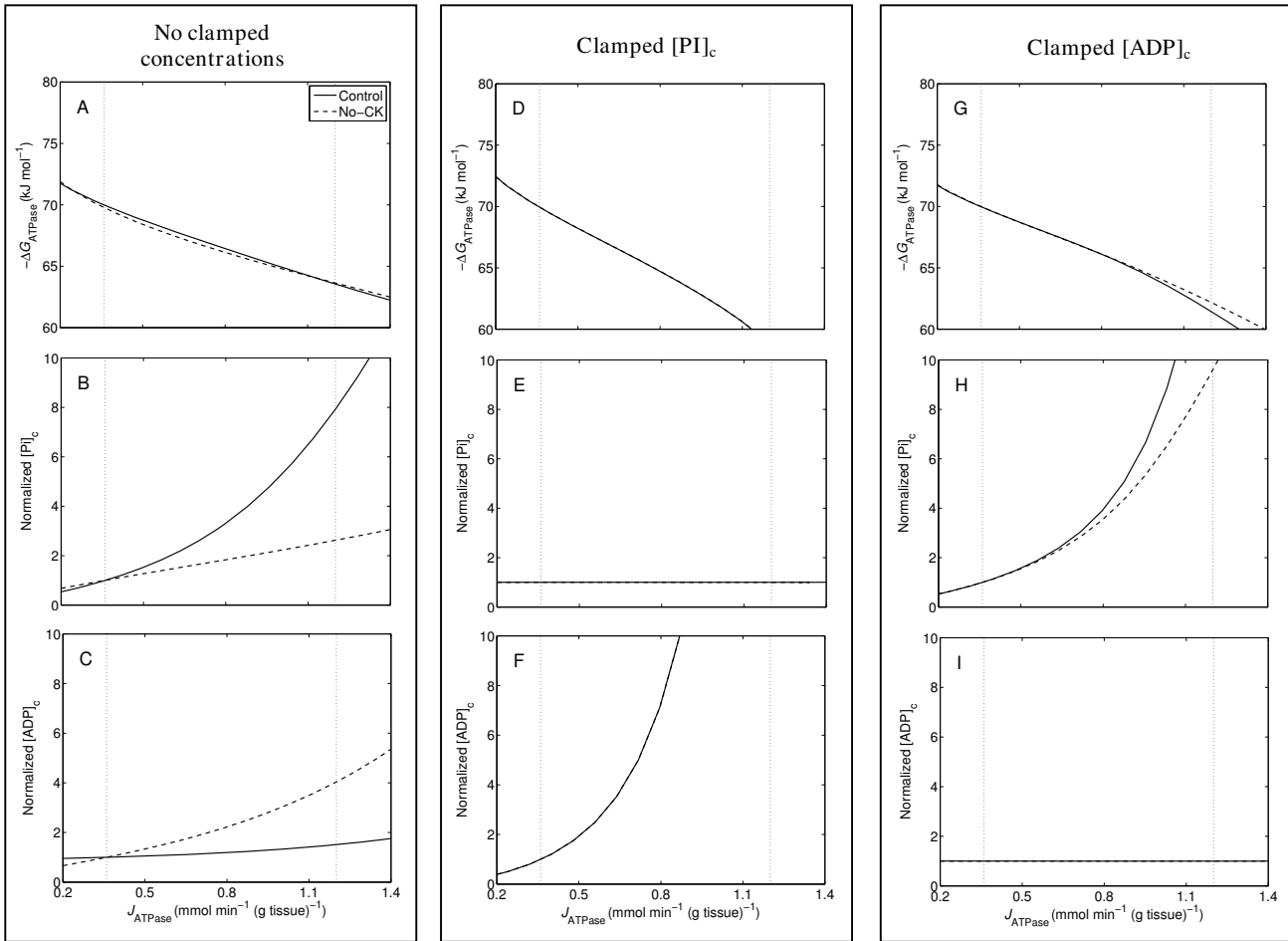


Figure 8
Steady-state average values of $-\Delta G_{ATPase}$, $[Pi]_c$, $[ADP]_c$, and $[CrP]_c$ plotted against ATP hydrolysis rate (J_{ATPase}).
 Model-predicted average values of $-\Delta G_{ATPase}$, normalized $[Pi]_c$, and normalized $[ADP]_c$ are plotted over the range of work rate with no clamped concentrations in A-C, with $[Pi]_c$ clamped in D-F, and with $[ADP]_c$ clamped in G-I. The model predictions are plotted as solid lines and dashed lines for the control and no-CK system, respectively. Model-predicted curves of the control and no-CK system overlap in D-F. The baseline and maximum hydrolysis rates, 0.36 and 1.2 $mmol\ s^{-1}\ (liter\ cell)^{-1}$, are indicated by vertical dotted lines.

$$\frac{d[CrP]_c}{d|\Delta G_{ATPase}|} = C. \tag{5}$$

Based on the simulations of $[CrP]_c$ and ΔG_{ATPase} at varying cardiac work rates in the normal system (illustrated in Figure 7), Equation (3) can be evaluated based on finite differences. The computed capacitance C is plotted Figure 9A against the normalized cytoplasmic CrP ($[CrP]_c/CR_{tot}$), where CR_{tot} is the total creatine pool in myocardium, 40.14 $mmol\ (l\ cytoplasm\ water)^{-1}$ [66]. As $[CrP]_c/CR_{tot}$ decreases from ~ 0.58 at the baseline work rate to ~ 0.48 at the maximum work rate, the value of C increases more

than three fold (from $\sim 0.33 \times 10^{-3}$ to $\sim 1.04 \times 10^{-3}\ mol\ l^{-1}\ kJ^{-1}$). As a result, the fluctuations of $|\Delta G_{ATPase}|$ (plotted as $\frac{\max(|\Delta G_{ATPase}|) - \min(|\Delta G_{ATPase}|)}{|\Delta G_{ATPase}|}$) decreases from $\sim 1.1\%$

to $\sim 0.55\%$, despite the increased range of oscillations of cytoplasmic ATP consumption rate. In contrast to the almost constant capacitance of the CK system determined for skeletal muscle [65], the CK system is predicted to increase in buffering capacity with work rate in the heart.

Other possible roles of the CK system

In addition to a temporal buffering function, the CK system has been proposed to facilitate transport of energetic phosphates in myocardium [7,19]. This hypothesis

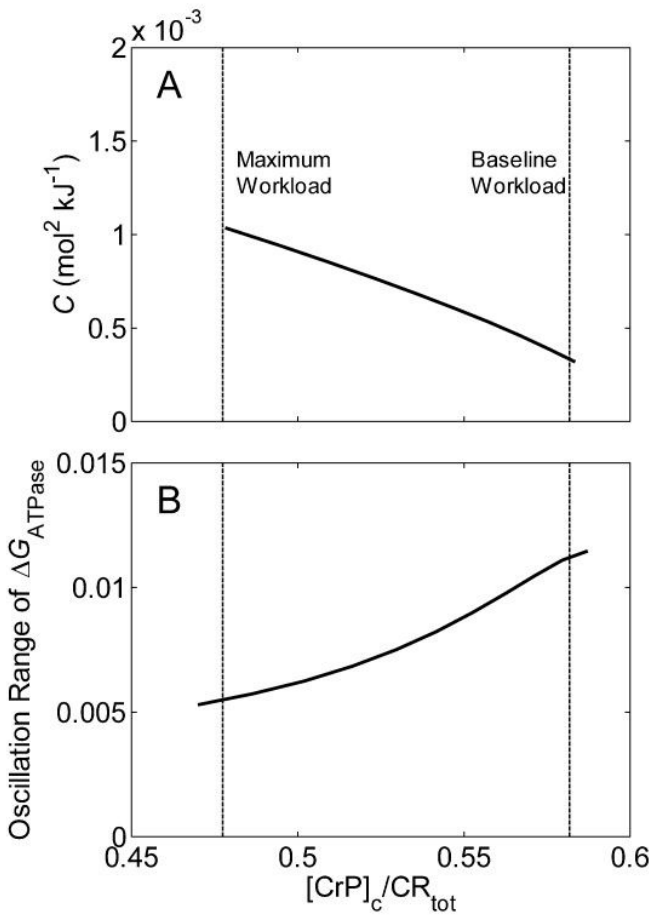


Figure 9
Buffer capacity of the CK system and range of oscillation of ΔG_{ATPase} plotted as functions of relative fractions of $[CrP]_c$. (A.) Capacitance of the CK system in buffering ΔG_{ATPase} , calculated from Equation (5), is plotted against $[CrP]_c/CR_{tot}$ predicted at different work rates. (B.) The predicted range of oscillation of ΔG_{ATPase} is plotted as $\frac{\max(|\Delta G_{ATPase}|) - \min(|\Delta G_{ATPase}|)}{|\Delta G_{ATPase}|}$. The curves in A and B are obtained by varying ATP hydrolysis rate from baseline ($0.36 \text{ mmol s}^{-1} (\text{l cell})^{-1}$) to maximum ($1.2 \text{ mmol s}^{-1} (\text{l cell})^{-1}$) values.

remains controversial. Meyer et al. [7] describe both temporal buffering and "spatial buffering" roles of creatine phosphate associated with the near-equilibrium creatine kinase (CK) reaction and a high cytoplasmic ATP-to-ADP ratio. The spatial buffering role may be negligible in the heart because of small diameters of cardiomyofibrils and abundant surrounding mitochondria [7]. The phospho-creatine shuttle hypothesis – that the free energy of ATP

hydrolysis is transported primarily by spatial gradients of CrP and Cr between mitochondria and sites of ATP hydrolysis – hinges on the existence of three critical phenomena: (1) restricted diffusion of adenine nucleotides in cardiomyocytes; (2) functional coupling (direct product-substrate channeling) between mitochondrial adenine nucleotide translocase and creatine kinase; and (3) disequilibrium of the CK reaction in cardiomyocytes [67-70]. While computational models that invoke these three phenomena are able to match data on the kinetics of oxidative phosphorylation in isolated skinned cardiomyocytes [71] and purified mitochondria [69], it remains to be demonstrated that the available data, particularly *in vivo* data, cannot be explained without invoking these phenomena. Indeed, recent measurements of diffusivities of labeled adenine nucleotides in cardiomyocytes demonstrate that bulk diffusion is not restricted to the degree necessary for the phosphocreatine shuttle to operate [72]. The existence and significance of "microcompartments" [69] around mitochondria with restricted diffusion in cardiomyocytes remains an active subject of investigation and debate.

Conclusion

To determine the roles of myoglobin and the CK system in stabilizing cardiac energy state, a computational model of oxygen transport and cardiac metabolism is applied to simulate transient changes and steady states in the beating heart. The analysis suggests that myoglobin has little impact on cardiac energetics, while the CK system is important for the beating heart to maintain stable energetic state over a range of cardiac work rate. Two distinct functions of the CK system are apparent from this analysis: first, the CK system buffers changes of $[ADP]_c$ and $[ATP]_c$ and ΔG_{ATPase} ; second, the CK system enhances the feedback of Pi to match the rate of mitochondrial ATP synthesis to cellular ATP demand while maintaining relatively stable $[ADP]_c$.

Authors' contributions

DAB and FW conceived and designed the experiments, carried out the experiments, and wrote the paper. Both authors read and approved the final manuscript.

Additional material

Additional file 1

Supplemental Material for "Roles of the creatine kinase system and myoglobin in maintaining energy state in the working heart". The supplemental material includes tables listing model components and detailed mathematical descriptions of the computational model.

Click here for file

[http://www.biomedcentral.com/content/supplementary/1752-0509-3-22-S1.doc]

Acknowledgements

The authors thank Drs. Kalyan C. Vinnakota, Feng Qi, and Martin J. Kushmerick for helpful discussions. This work was supported by NIH grant HL072011 (DAB).

References

- Guyton AC, Hall JE: *Textbook of Medical Physiology* 10th edition. Philadelphia: W. B. Saunders Company; 2000.
- Katz AM: *Physiology of the heart* 4th edition. Philadelphia: Lippincott Williams & Wilkins; 2006.
- Millikan G: **Muscle hemoglobin.** *Physiological Reviews* 1939, **19**:503-523.
- Wittenberg JB: **Myoglobin-facilitated oxygen diffusion: role of myoglobin in oxygen entry into muscle.** *Physiol Rev* 1970, **50**:559-636.
- Ordway GA, Garry DJ: **Myoglobin: an essential hemoprotein in striated muscle.** *J Exp Biol* 2004, **207**:3441-3446.
- Jurgens KD, Papadopoulos S, Peters T, Gros G: **Myoglobin: Just an Oxygen Store or Also an Oxygen Transporter?** *News Physiol Sci* 2000, **15**:269-274.
- Meyer RA, Sweeney HL, Kushmerick MJ: **A simple analysis of the "phosphocreatine shuttle".** *Am J Physiol* 1984, **246**:C365-377.
- Wallimann T, Wyss M, Brdiczka D, Nicolay K, Eppenberger HM: **Intracellular compartmentation, structure and function of creatine kinase isoenzymes in tissues with high and fluctuating energy demands: the 'phosphocreatine circuit' for cellular energy homeostasis.** *Biochem J* 1992, **281**(Pt 1):21-40.
- Papadopoulos S, Endeward V, Revesz-Walker B, Jurgens KD, Gros G: **Radial and longitudinal diffusion of myoglobin in single living heart and skeletal muscle cells.** *Proc Natl Acad Sci USA* 2001, **98**:5904-5909.
- Murray JD: **On the role of myoglobin in muscle respiration.** *J Theor Biol* 1974, **47**:115-126.
- Wittenberg BA, Wittenberg JB, Caldwell PR: **Role of myoglobin in the oxygen supply to red skeletal muscle.** *J Biol Chem* 1975, **250**:9038-9043.
- Wyman J: **Facilitated diffusion and the possible role of myoglobin as a transport mechanism.** *J Biol Chem* 1966, **241**:115-121.
- Frauenfelder H, McMahon BH, Austin RH, Chu K, Groves JT: **The role of structure, energy landscape, dynamics, and allostery in the enzymatic function of myoglobin.** *Proc Natl Acad Sci USA* 2001, **98**:2370-2374.
- Rassaf T, Fogel U, Drexhage C, Hendgen-Cotta U, Kelm M, Schrader J: **Nitrite reductase function of deoxymyoglobin: oxygen sensor and regulator of cardiac energetics and function.** *Circ Res* 2007, **100**:1749-1754.
- Kreutzer U, Jue T: **Role of myoglobin as a scavenger of cellular NO in myocardium.** *Am J Physiol Heart Circ Physiol* 2004, **286**:H985-991.
- Schlattner U, Tokarska-Schlattner M, Wallimann T: **Mitochondrial creatine kinase in human health and disease.** *Biochimica Et Biophysica Acta-Molecular Basis of Disease* 2006, **1762**:164-180.
- Beard DA, Schenkman KA, Feigl EO: **Myocardial oxygenation in isolated hearts predicted by an anatomically realistic microvascular transport model.** *Am J Physiol Heart Circ Physiol* 2003, **285**:H1826-1836.
- Zhang J, Murakami Y, Zhang Y, Cho YK, Ye Y, Gong G, Bache RJ, Ugurbil K, From AH: **Oxygen delivery does not limit cardiac performance during high work states.** *Am J Physiol* 1999, **277**:H50-57.
- Saks VA, Kongas O, Vendelin M, Kay L: **Role of the creatine/phosphocreatine system in the regulation of mitochondrial respiration.** *Acta Physiologica Scandinavica* 2000, **168**:635-641.
- Saks VA, Ventura-Clapier R, Aliev MK: **Metabolic control and metabolic capacity: two aspects of creatine kinase functioning in the cells.** *Biochim Biophys Acta* 1996, **1274**:81-88.
- Wu F, Zhang EY, Zhang J, Bache RJ, Beard DA: **Phosphate metabolite concentrations and ATP hydrolysis potential in normal and ischemic hearts.** *J Physiol* 2008, **586**:4193-4208.
- Beard DA: **Modeling of oxygen transport and cellular energetics explains observations on in vivo cardiac energy metabolism.** *PLoS Comput Biol* 2006, **2**:e107.
- Wu F, Yang F, Vinnakota KC, Beard DA: **Computer modeling of mitochondrial tricarboxylic acid cycle, oxidative phosphorylation, metabolite transport, and electrophysiology.** *J Biol Chem* 2007, **282**:24525-24537.
- Zhang J, From AH, Ugurbil K, Bache RJ: **Myocardial oxygenation and high-energy phosphate levels during KATP channel blockade.** *Am J Physiol Heart Circ Physiol* 2003, **285**:H1420-1427.
- Zhang J, Gong G, Ye Y, Guo T, Mansoor A, Hu Q, Ochiai K, Liu J, Wang X, Cheng Y, et al.: **Nitric oxide regulation of myocardial O₂ consumption and HEP metabolism.** *Am J Physiol Heart Circ Physiol* 2005, **288**:H310-316.
- Gong G, Liu J, Liang P, Guo T, Hu Q, Ochiai K, Hou M, Ye Y, Wu X, Mansoor A, et al.: **Oxidative capacity in failing hearts.** *Am J Physiol Heart Circ Physiol* 2003, **285**:H541-548.
- Ochiai K, Zhang J, Gong G, Zhang Y, Liu J, Ye Y, Wu X, Liu H, Murakami Y, Bache RJ, et al.: **Effects of augmented delivery of pyruvate on myocardial high-energy phosphate metabolism at high workload.** *Am J Physiol Heart Circ Physiol* 2001, **281**:H1823-1832.
- Gong G, Ugurbil K, Zhang J: **Transmural metabolic heterogeneity at high cardiac work states.** *Am J Physiol* 1999, **277**:H236-242.
- Bache RJ, Zhang J, Murakami Y, Zhang Y, Cho YK, Merkle H, Gong G, From AH, Ugurbil K: **Myocardial oxygenation at high work states in hearts with left ventricular hypertrophy.** *Cardiovasc Res* 1999, **42**:616-626.
- Rooke GA, Feigl EO: **Work as a correlate of canine left ventricular oxygen consumption, and the problem of catecholamine oxygen wasting.** *Circ Res* 1982, **50**:273-286.
- Vinnakota KC, Wu F, Kushmerick MJ, Beard DA: **Multiple Ion Binding Equilibria, Reaction Kinetics and Thermodynamics in Dynamic Models of Biochemical Pathways.** *Methods in Enzymology* 2009:29-68.
- Murray JD: *Mathematical biology* 3rd edition. New York: Springer; 2002.
- Kushmerick MJ: **Energy balance in muscle activity: simulations of ATPase coupled to oxidative phosphorylation and to creatine kinase.** *Comp Biochem Physiol B Biochem Mol Biol* 1998, **120**:109-123.
- Neubauer S: **The failing heart – an engine out of fuel.** *N Engl J Med* 2007, **356**:1140-1151.
- Drabkin DL: **The Distribution of the Chromoproteins, Hemoglobin, Myoglobin, and Cytochrome C, in the Tissues of Different Species, and the Relationship of the Total Content of Each Chromoprotein to Body Mass.** *J Biol Chem* 1950, **182**:317-334.
- Lin L, Sylven C, Sotonyi P, Somogyi E, Kaijser L, Jansson E: **Myoglobin content and citrate synthase activity in different parts of the normal human heart.** *J Appl Physiol* 1990, **69**:899-901.
- Garry DJ, Kanatous SB, Mammen PP: **Emerging roles for myoglobin in the heart.** *Trends Cardiovasc Med* 2003, **13**:111-116.
- Kooyman GL, Ponganis PJ: **The physiological basis of diving to depth: birds and mammals.** *Annu Rev Physiol* 1998, **60**:19-32.
- Riveros-Moreno V, Wittenberg JB: **The self-diffusion coefficients of myoglobin and hemoglobin in concentrated solutions.** *J Biol Chem* 1972, **247**:895-901.
- Federspiel WJ: **A model study of intracellular oxygen gradients in a myoglobin-containing skeletal muscle fiber.** *Biophys J* 1986, **49**:857-868.
- Papadopoulos S, Jurgens KD, Gros G: **Protein diffusion in living skeletal muscle fibers: dependence on protein size, fiber type, and contraction.** *Biophys J* 2000, **79**:2084-2094.
- Beard DA, Bassingthwaite JB: **Modeling advection and diffusion of oxygen in complex vascular networks.** *Ann Biomed Eng* 2001, **29**:298-310.
- Lin PC, Kreutzer U, Jue T: **Anisotropy and temperature dependence of myoglobin translational diffusion in myocardium: implication for oxygen transport and cellular architecture.** *Biophys J* 2007, **92**:2608-2620.
- Lin PC, Kreutzer U, Jue T: **Myoglobin translational diffusion in rat myocardium and its implication on intracellular oxygen transport.** *J Physiol* 2007, **578**:595-603.
- Timmons JA, Gustafsson T, Sundberg CJ, Jansson E, Greenhaff PL: **Muscle acetyl group availability is a major determinant of oxygen deficit in humans during submaximal exercise.** *Am J Physiol* 1998, **274**:E377-380.
- Timmons JA, Poucher SM, Constantin-Teodosiu D, Worrall V, Macdonald IA, Greenhaff PL: **Increased acetyl group availability**

- enhances contractile function of canine skeletal muscle during ischemia. *J Clin Invest* 1996, **97**:879-883.**
47. Fogel U, Merx MW, Godecke A, Decking UK, Schrader J: **Myoglobin: A scavenger of bioactive NO.** *Proc Natl Acad Sci USA* 2001, **98**:735-740.
 48. Garry DJ, Ordway GA, Lorenz JN, Radford NB, Chin ER, Grange RW, Bassel-Duby R, Williams RS: **Mice without myoglobin.** *Nature* 1998, **395**:905-908.
 49. Godecke A, Fogel U, Zanger K, Ding Z, Hirchenhain J, Decking UK, Schrader J: **Disruption of myoglobin in mice induces multiple compensatory mechanisms.** *Proc Natl Acad Sci USA* 1999, **96**:10495-10500.
 50. Cooke JP, Losordo DW: **Nitric oxide and angiogenesis.** *Circulation* 2002, **105**:2133-2135.
 51. Al-Ani B, Hewett PW, Ahmed S, Cudmore M, Fujisawa T, Ahmad S, Ahmed A: **The release of nitric oxide from S-nitrosothiols promotes angiogenesis.** *PLoS ONE* 2006, **1**:e25.
 52. Zhang R, Wang L, Zhang L, Chen J, Zhu Z, Zhang Z, Chopp M: **Nitric oxide enhances angiogenesis via the synthesis of vascular endothelial growth factor and cGMP after stroke in the rat.** *Circ Res* 2003, **92**:308-313.
 53. Fogel U, Laussmann T, Godecke A, Abanador N, Schafers M, Fingas CD, Metzger S, Levkau B, Jacoby C, Schrader J: **Lack of myoglobin causes a switch in cardiac substrate selection.** *Circ Res* 2005, **96**:e68-75.
 54. Nelson DL, Cox MM: *Lehninger Principles of Biochemistry* 4th edition. New York: W. H. Freeman and Company; 2005.
 55. Quyyumi AA, Dakak N, Andrews NP, Gilligan DM, Panza JA, Cannon RO 3rd: **Contribution of nitric oxide to metabolic coronary vasodilation in the human heart.** *Circulation* 1995, **92**:320-326.
 56. Joannides R, Haefeli WE, Linder L, Richard V, Bakkali EH, Thuillez C, Luscher TF: **Nitric oxide is responsible for flow-dependent dilatation of human peripheral conduit arteries in vivo.** *Circulation* 1995, **91**:1314-1319.
 57. Balaban RS: **Modeling mitochondrial function.** *Am J Physiol Cell Physiol* 2006, **291**:C1107-1113.
 58. Bose S, French S, Evans FJ, Joubert F, Balaban RS: **Metabolic network control of oxidative phosphorylation: multiple roles of inorganic phosphate.** *J Biol Chem* 2003, **278**:39155-39165.
 59. Wu F, Jeneson JA, Beard DA: **Oxidative ATP synthesis in skeletal muscle is controlled by substrate feedback.** *Am J Physiol Cell Physiol* 2007, **292**:C115-124.
 60. Beard DA: **A Biophysical Model of the Mitochondrial Respiratory System and Oxidative Phosphorylation.** *PLoS Comput Biol* 2005, **1**:e36.
 61. Saupé KVV, Spindler M, Tian R, Ingwall JS: **Impaired cardiac energetics in mice lacking muscle-specific isoenzymes of creatine kinase.** *Circ Res* 1998, **82**:898-907.
 62. Kushmerick MJ, Moerland TS, Wiseman RW: **Mammalian skeletal muscle fibers distinguished by contents of phosphocreatine, ATP, and Pi.** *Proc Natl Acad Sci USA* 1992, **89**:7521-7525.
 63. Kushmerick MJ, Meyer RA, Brown TR: **Regulation of oxygen consumption in fast- and slow-twitch muscle.** *Am J Physiol* 1992, **263**:C598-606.
 64. Chance B, Leigh JS Jr, Clark BJ, Maris J, Kent J, Nioka S, Smith D: **Control of oxidative metabolism and oxygen delivery in human skeletal muscle: a steady-state analysis of the work/energy cost transfer function.** *Proc Natl Acad Sci USA* 1985, **82**:8384-8388.
 65. Meyer RA: **A linear model of muscle respiration explains monoexponential phosphocreatine changes.** *Am J Physiol* 1988, **254**:C548-553.
 66. Katz LA, Swain JA, Portman MA, Balaban RS: **Relation between phosphate metabolites and oxygen consumption of heart in vivo.** *Am J Physiol* 1989, **256**:H265-274.
 67. Vendelin M, Beraud N, Guerrero K, Andrienko T, Kuznetsov AV, Olivares J, Kay L, Saks V: **Mitochondrial regular arrangement in muscle cells: a "crystal-like" pattern.** *Journal of Physiology* 2004, **288**(3):C757-C767.
 68. Vendelin M, Kongas O, Saks V: **Regulation of mitochondrial respiration in heart cells analyzed by reaction-diffusion model of energy transfer.** *Am J Physiol Cell Physiol* 2000, **278**(4):C747-7C64.
 69. Vendelin M, Lemba M, Saks VA: **Analysis of functional coupling: mitochondrial creatine kinase and adenine nucleotide translocase.** *Biophys J* 2004, **87**:696-713.
 70. Saks VA, Kuznetsov AV, Vendelin M, Guerrero K, Kay L, Seppet EK: **Functional coupling as a basic mechanism of feedback regulation of cardiac energy metabolism.** *Mol Cell Biochem* 2004, **256-257**:185-199.
 71. Vendelin M, Eimre M, Seppet E, Peet N, Andrienko T, Lemba M, Engelbrecht J, Seppet EK, Saks VA: **Intracellular diffusion of adenosine phosphates is locally restricted in cardiac muscle.** *Mol Cell Biochem* 2004, **256-257**:229-241.
 72. Vendelin M, Birkedal R: **Anisotropic diffusion of fluorescently labeled ATP in rat cardiomyocytes determined by raster image correlation spectroscopy.** *Am J Physiol Cell Physiol* 2008.

Publish with **BioMed Central** and every scientist can read your work free of charge

"BioMed Central will be the most significant development for disseminating the results of biomedical research in our lifetime."

Sir Paul Nurse, Cancer Research UK

Your research papers will be:

- available free of charge to the entire biomedical community
- peer reviewed and published immediately upon acceptance
- cited in PubMed and archived on PubMed Central
- yours — you keep the copyright

Submit your manuscript here:
http://www.biomedcentral.com/info/publishing_adv.asp

